AIP Advances

Inhibition of the ultrasonic microjet-pits on the carbon steel in the particles-water mixtures

Dayun Yan, Jiadao Wang, and Fengbin Liu

Citation: AIP Advances **5**, 077159 (2015); doi: 10.1063/1.4927505
View online: http://dx.doi.org/10.1063/1.4927505
View Table of Contents: http://scitation.aip.org/content/aip/journal/adva/5/7?ver=pdfcov
Published by the AIP Publishing

Inhibition of the ultrasonic microjet-pits on the carbon steel in the particles-water mixtures

Dayun Yan,[1] Jiadao Wang,[2,a] and Fengbin Liu[3]
[1]*Department of Mechanical and Aerospace Engineering, The George Washington University, Washington, District of Columbia, United States of America, 20052*
[2]*State Key Laboratory of Tribology, Tsinghua University, Beijing, P.R. China, 100084*
[3]*College of Mechanical & Electric Engineering, North China University of Technology, Beijing, P.R. China, 100144*

(Received 25 May 2015; accepted 15 July 2015; published online 23 July 2015)

In the incubation period of ultrasonic cavitation, due to the impact of microjets on the material surface, the needle-like microjet-pits are formed. Because the formation of microjet-pits relates with the evolution of cavitation erosion on engineering materials, corresponding study will promote the understanding on the mechanism of cavitation erosion. However, little study on the microjet-pits has been carried out, especially in the particles-water mixture. In this study, we firstly demonstrated the microjet-pits on the carbon steel would be significantly inhibited by Al particles in water. Such inhibition effect indicated that particular particles might not only provide growth sites for cavitation bubbles but also affect the collapse of cavitation bubbles near a solid surface. Our study deepened the understanding on the ultrasonic cavitation erosion in the particles-water mixture. [http://dx.doi.org/10.1063/1.4927505]

I. INTRODUCTION

In the ultrasonic cavitation, the oscillation of pressure in water breaks the attractive hydrogen bond interaction among water molecules and form cavitation bubbles.[1] Despite the theoretical tensile strength of water is about 1000 bar, due to the existence of inhomogeneities in the water, the measured value (on the order of 1bar) is much lower than the theoretical value.[2] The pockets of gases stabilized at the bottom of cracks or crevices on impurities serve as the weak points that prevented water from sustaining a large tensile strength.[2,3] For the water-particles mixture, the gas nuclei in crevices on the surface of particle grow into cavitation bubbles when they are irradiated by the ultrasound wave.[4,5] Therefore, in contrast to the pure water, the cavitation threshold of particles-water mixture is decreased, which results in an increased cavitation level.[6,7] Meanwhile, because the cavitation erosion is due to the collapse of cavitation bubbles, the particles-water mixture causes stronger cavitation erosion than the pure water does. Chen et al.[1,8] reported that both CeO_2 particles and SiO_2 particles enhanced the ultrasonic cavitation erosion on stainless steel. Huang et al.[9] discovered that the ultrasonic cavitation erosion occurred in the solid-water mixtures were more significant than that occurred in the pure water. Recently, Zmij et al.[10] applied B_4C particles to enhance the ultrasonic cavitation erosion in the resistance tests on a coated steel.

For the incubation period of ultrasonic cavitation erosion on engineering materials (stainless steel, brass, and aluminum), two types damage are formed. One is the microjet-pit, which is due to the highly erosive microjet with the impact of stress larger than the strength of specimen.[11] Another is the shockwave-pit, which is attributed to the plastic flow of surface material under the impact of shockwave.[11] The microjet-pits are found to be smaller in size and are deeper compared with the shockwave-pits.[11] Because the microjet-pits directly relate to the impact of microjet, the study

[a]Corresponding authors. Jiadao Wang: jdwang@mail.tsinghua.edu.cn

focusing on the microjet-pits will definitely reveal more details about the collapse of cavitation bubbles and the mechanism of cavitation erosion. Currently, the study focusing on the microjet-pits is lacking, particularly for the case in the particles-water mixture. Whether the particles in mixture will definitely generate more microjet-pits on carbon steel is still unknown.

Because the size of microjet-pits is just about several micrometers,[11] it is not practical to measure the weight loss owing to the formation of microjet-pits in the incubation period by electronic balances which are always harnessed to characterize the cavitation erosion stage. In addition, it is also hard to distinguish the microjet-pits on many engineering materials via using electron scanning microscope under low resolution. However, due to corrosion effect, for carbon steel, including AISI1045[12] and ASTM A283,[13] the microjet-pit is always surrounded by a ring area with a size much larger than the microjet-pit. As a result, it is convenient to investigate the generation of microjet-pits using SEM under low resolution, which enables us to scan a relative large area on the carbon steel.

The amount of microjet-pits directly reflects the ultrasonic cavitation level. To characterize the cavitation level in the particles-water mixture, methylene blue (MB) was harnessed as the sonochemical indicator. MB solution changes from blue into colorless when MB reacts with hydroxyl free radicals generated in the collapse of cavitation bubbles.[14] The declined absorbency of the absorption spectrum of MB solution characterizes the ultrasonic cavitation level.[15] MB has been used to characterize the hydroxyl free radicals induced in Venturi cavitation flow.[16] Besides, different from saline solutions (such as NaCl) which induces the noticeable corrosion on carbon steel,[17] MB shows the corrosion inhibition effect on carbon steel.[18] Ultimately, the underlying mechanism was discussed. This study provided an approach to study the ultrasonic cavitation erosion merely due to the attack of shockwaves, which would facilitate the research on the mechanism of cavitation erosion.

II. METHODS AND EXPERIMENTS

The schematic of ultrasound irradiation device is shown in Fig. 1(a). The titanium horn with a tip diameter of 15 mm driven by the piezoelectric transducer oscillated to generate ultrasound wave in water to induce the cavitation. The cavitation erosion occurred on the specimen screwed at the tip of horn. The frequency and the power of piezoelectric transducer were 20 KHz and 400W, respectively. A beaker containing 200 mL aqueous solution was under the horn. The distance between the

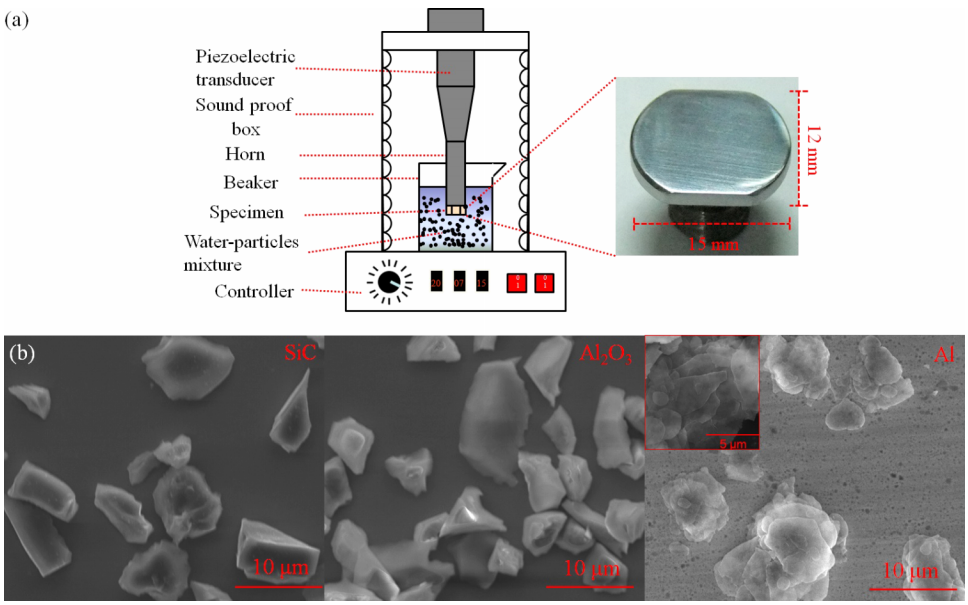

FIG. 1. Experimental set up (a) and SEM images of particles (b).

surface of specimen and the base of beaker was 20 mm. The photo of specimen is shown in the right inset of Fig. 1(a). The specimen was made of AISI 1045 steel. Its surface has been polished with a surface roughness of Ra 43.3 nm.

The SEM images of SiC particles, Al_2O_3 particles, and Al particles are shown in Fig. 1(b). The nominal sizes of all particles were 5 μm. The real sizes were characterized by Laser Particle Size and Potential Analyzer (ZETA3000HS). Corresponding mean size was 5.5 μm, 5.5 μm, and 7.5 μm, respectively. The surfaces of SiC particles and Al_2O_3 particles were smooth. In contrast, the surfaces of Al particles were rough and lamellar. Noticeable nano scale crevices appeared on the surfaces of Al particles (the inset in Fig. 1(b)), which were due to their unique structures that each Al particle was piled up with tens of thin sheets.

The experimental protocols are illustrated as following. First of all, the ultrasonic cavitation was performed in deionized water. Then, experiments were performed in four 0.05 wt% particles-water mixtures containing different kinds of particles, respectively. In each experiment, the horn oscillated 15 times with each time lasting 20 s. The interval time between two oscillations was 7 s. The total ultrasonic oscillating time was 5 min. When experiments ended, specimens were washed by ethanol to avoid rusting. The cavitation erosion on the surface of carbon steel was characterized using SEM.

Similarly, to qualify the ultrasonic cavitation level, the same experiments were performed in the MB solution and particles-MB solution mixtures again. 8 mM MB solutions were prepared by dissolving MB powders in deionized water with the electromagnetic stirring for 10 min. After the ultrasonic cavitation, the particles-MB solution mixtures were centrifuged for 10 min by the ultracentrifuge at a speed of 15000 rpm. The particles precipitated at the bottom of centrifuge tube. 10 mL upper layer pellucid MB solution in centrifuge tube was collected. Furthermore, 10 mL initial pure MB solution and 10 mL pure MB solution undergone experiment were also collected, respectively. Ultimately, collected MB solutions were characterized using Ultraviolet-Visible Spectrophotometer (HP HEWLETT Packard 8425).

III. RESULTS AND DISCUSSION

In contrast to deionized water, the appearance of ultrasonic microjet-pits on carbon steel can be enhanced or completely repressed in particular particles-water mixtures. As shown in SEM images, large amount of white circular spots with black needle-like centers appear on the carbon steel upon the ultrasonic cavitation in deionized water (Fig. 2(a)), SiC-water mixture (Fig. 2(b)), and Al_2O_3-water mixture (Fig. 2(c)). By contrast, almost no similar white spots appear on the carbon steel upon the ultrasonic cavitation in Al-water mixture (Fig. 2(d)). Other than these damage morphologies, the plastic protuberances noticeably appear on surfaces of all specimens experienced the ultrasonic cavitation. Interlaced plastic protuberances form net-like structures covering the whole surface of carbon steel.

To better investigate these two material deformations upon the ultrasonic cavitation, the slant observation model of SEM was used. The specimen holder was tilted to form an angle of 60° between the normal of the specimen surface and the axis of electronic gun in SEM. As shown in Fig. 2(e), the protuberant feature of the plastic deformation and the sunken feature of microjet-pits are clearly illustrated simultaneously. The black central dot in the white circular spot shown in Fig. 2(a), 2(b), and 2(c) actually is an ultrasonic microjet-pit surrounded by a ring area consisted of irregular oxide structures. The diameter of the microjet-pit and its peripheral ring area are about 2 μm and 20 μm, respectively. A cut on the microje-pit by Focused Ion Beam (FIB) revealed that the depth of pit was about 5 μm (the upper-right inset in Fig. 2(e)). Considering the morphology similarity among the vibratory cavitation erosion on other materials (stainless steel, brass, aluminum), the plastic protuberance should be caused by the plastic flow of material under the impact of shockwave generated in the collapse of cavitation bubble.[11] Liu et al.[19] observed the similar plastic protuberances on the surface of carbon steel upon the ultrasonic cavitation. They pointed out that the plastic protuberances and the surfaces encircled by protuberances were ferrite phases and pearlite phases in carbon steel, respectively.[19] Because of the mechanical strength of ferrite phase

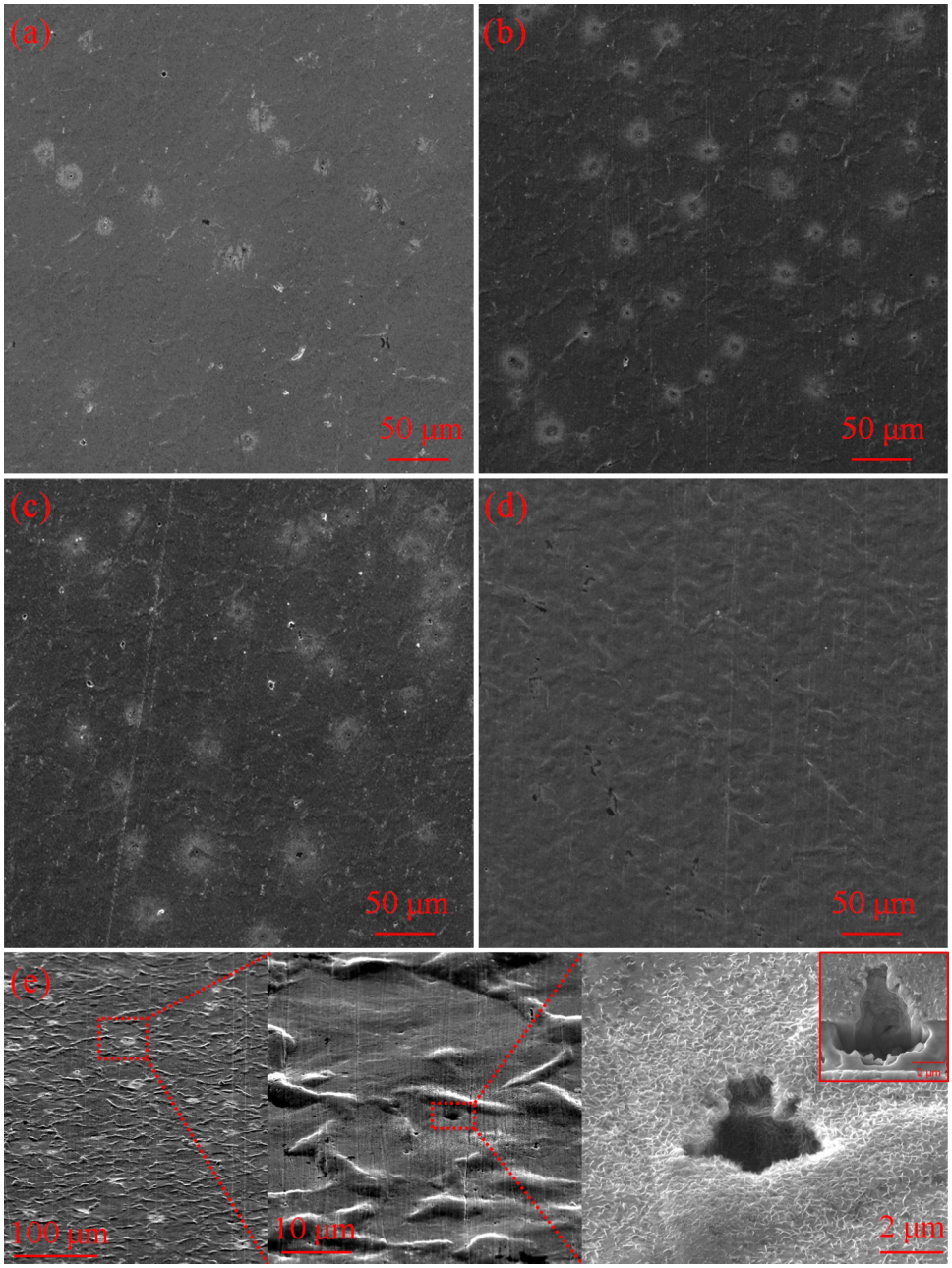

FIG. 2. SEM images of carbon steel surface after the ultrasonic cavitation in (a) deionized water, (b) SiC-water mixture, (c) Al_2O_3-water mixture, and (d) Al-water mixture. (e) Slant observation on the carbon steel upon the ultrasonic cavitation in deionized water.

was lower than that of pearlite phase, the plastic deformation tended to occur on ferrite phase and forced it bulged up.[19]

Al particles are able to depress the generation of microjet-pits even other particles co-exist in the mixture. We further investigated the generation of microjet-pits on carbon steel upon the ultrasonic cavitation in the hybrid particles-water mixture, which was prepared by mixing 0.1 g SiC particles or Al_2O_3 particles (5 μm) with 0.1 g Al particles (5 μm) in the 200 mL deionized water. The ultrasonic oscillating time of each case was 5 min. As demonstrated above, both SiC particles and Al_2O_3 particles are able to enhance the microjet-pits number on the carbon steel. However, it was found that Al particles disable SiC particles' power by inhibiting almost all microjet-pits

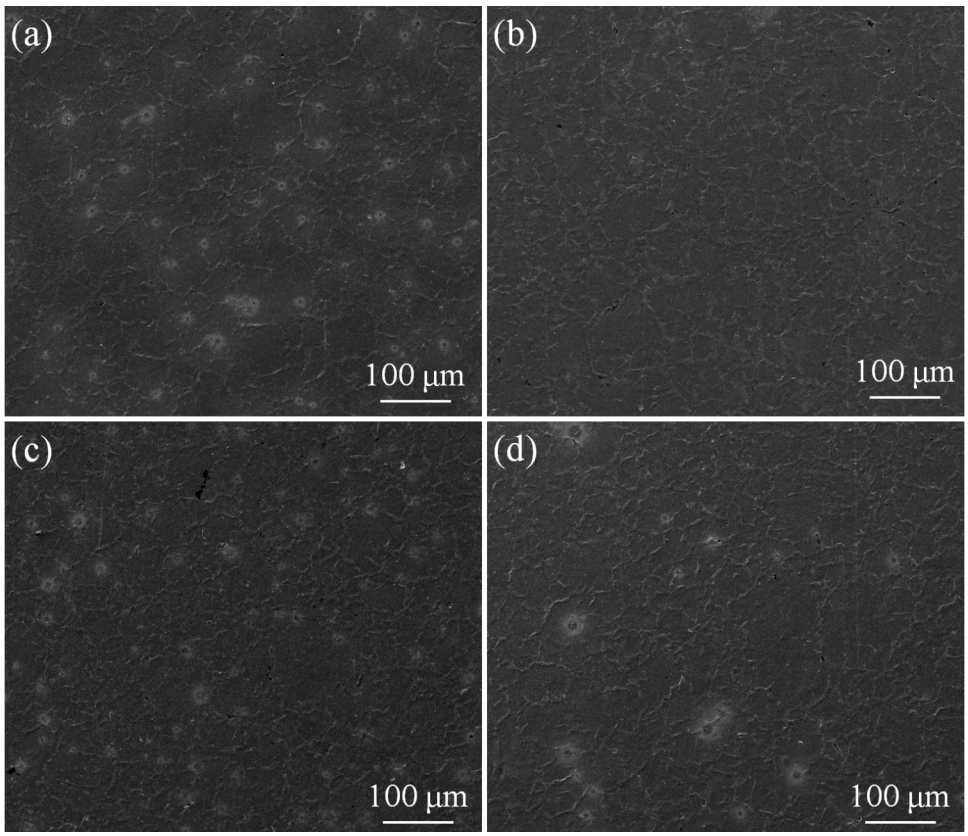

FIG. 3. SEM of the carbon steel upon the ultrasonic cavitation. (a) SiC (0.05wt%)-water mixture. (b) SiC (0.05wt%)/Al (0.05wt%)-water mixture. (c) Al_2O_3 (0.05wt%)-water mixture. (d) Al_2O_3 (0.05wt%)/Al (0.05wt%)-water mixture.

appeared on the carbon steel (Fig. 3(a), 3(b)) albeit the net-like plastic protuberances still appeared on the carbon steel (Fig. 3(b)). However, Al particles would only partially inhibit the microjet-pits when Al_2O_3 particles exist in the mixture (Fig. 3(c), 3(d)). Similarly, the net-like plastic protuberances (Fig. 3(d)) have not been affected by Al particles. Above phenomena indicate that the anti microjet-pits capacity of Al particles may relate with its unique chemical property, which is absent on SiC particles and Al_2O_3 particles.

In the hybrid particles-water mixture, the anti microjet-pits capacity of Al particles is also affected by the relative amount of Al particles to other particles. We investigated the anti microjet-pits capacity of Al (5 μm)/SiC (2.5 μm)-water mixture upon the ultrasonic cavitation. Specifically, we prepared 1:1 and 3:1 hybrid particles-water mixtures by mixing 0.1 g Al particles with 0.1 g SiC particles and mixing 0.3 g Al particles with 0.1 g SiC particles in the 200 mL deionized water, respectively. The ultrasonic oscillating time of each case was 5 min. When the whole mass of particles is fixed, the size of particles is inverse proportional to the number of particles. Thus, in contrast to the ultrasonic cavitation performed in SiC (5 μm)-water mixture (Fig. 2(b)), more microjet-pits was found on the carbon steel when the ultrasonic cavitation was performed in SiC (2.5 μm)-water mixture (Fig. 4(a)). When the mass ratio of Al particles to SiC particles was 1, significant microjet-pits still generated on the carbon steel (Fig. 4(b)). However, when the mass ratio of Al particles to SiC particles increased to 3, no microjet-pits appeared on the carbon steel (Fig. 4(c)).

The plastic protuberances on the carbon steel are not inhibited by Al particles. We investigated the evolution of carbon steel surface after the ultrasonic cavitation in 0.05 wt% Al-water mixture. As shown in Fig. 5, even the experiment lasts 20 min, the microjet-pits do not appear on the carbon steel. In contrast, as the time of ultrasonic irradiation increases, the plastic protuberances gradually from and become distinguishable on the carbon steel. Other than the plastic protuberances, the

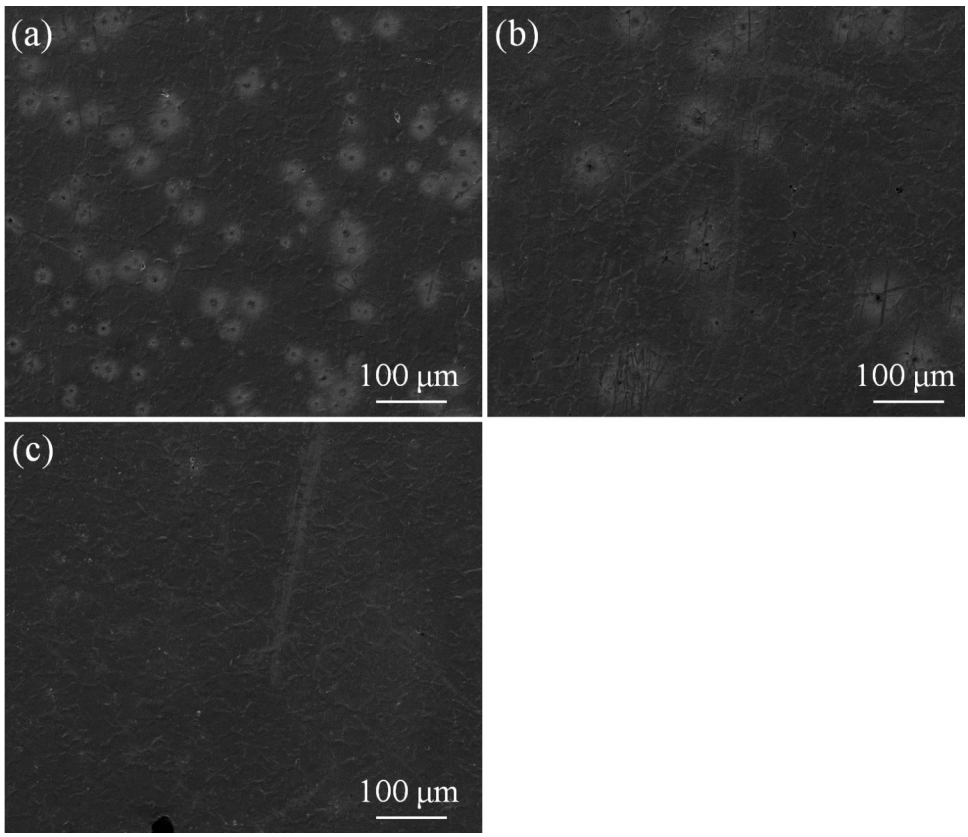

FIG. 4. SEM of the carbon steel upon the ultrasonic cavitation. (a) SiC 2.5 μm (0.05wt%)-water mixture. (b) SiC 2.5 μm (0.05wt%)/Al 2.5 μm (0.05wt%)-water mixture. (c) SiC 2.5 μm (0.05wt%)/Al 2.5 μm (0.15wt%)-water mixture.

surface of carbon steel encircled by the net-like plastic protuberances also significantly varies over the 20 min of ultrasonic cavitation. As shown in the left bottom inset of Fig. 5, the smooth surface encircled by the plastic protuberances has been replaced with the lamellar structures. The original material in the gaps of lamellar structures has been lost in the ultrasonic cavitation. Leu et al.[19]

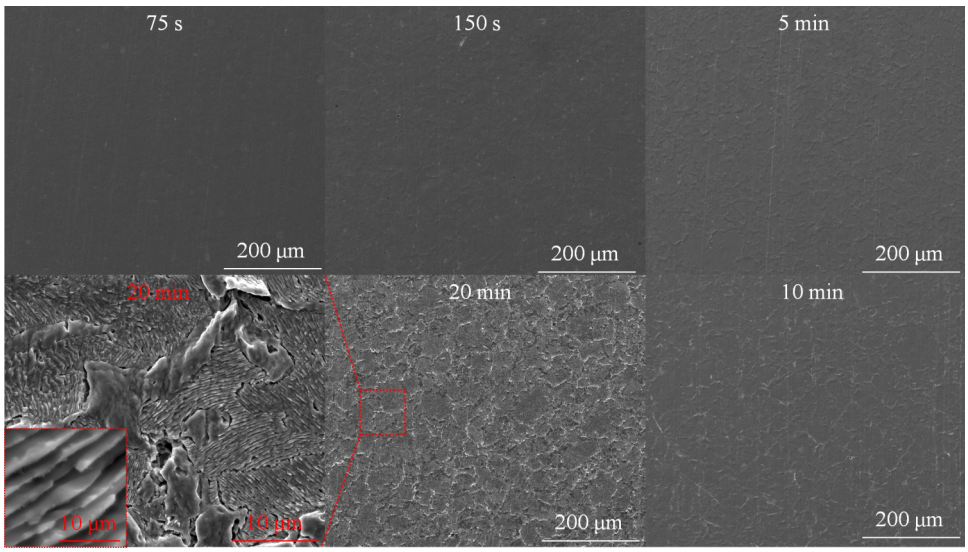

FIG. 5. The time-lapse SEM images of carbon steel after the ultrasonic cavitation performed in 0.05 wt% Al-H_2O mixture.

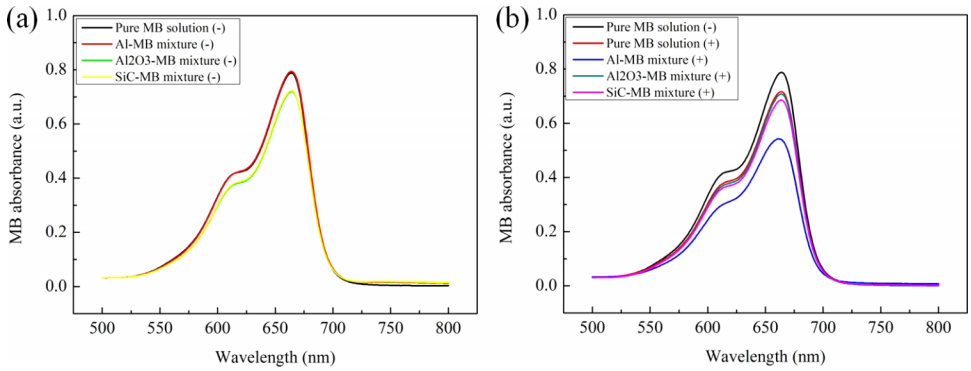

FIG. 6. Absorption spectra of MB solution and particles-MB mixtures without (a) and with (b) the ultrasonic cavitation.

proposed that the lamellar structures were formed by the loss of cementite phase in pearlite phase due to the continuous shockwave impact on pearlite phase during ultrasonic cavitation erosion.

Furthermore, the ultrasonic cavitation level in the particles-H_2O mixture demonstrates that Al particles significantly enhance the ultrasonic cavitation level in water. Despite MB molecules slightly absorb on Al_2O_3 particles and SiC particles, no absorption of MB on Al particles has been found (Fig. 6(a)). Comparing the absorption curves in Fig. 6(a) and Fig. 6(b), we found that only the absorbance at 664 nm of MB solutions from Al-MB mixture significantly declined upon the ultrasonic cavitation. SiC particles and Al_2O_3 particles slightly and does not increase the ultrasonic cavitation after experiment, respectively. For the experiment performed in the pure MB solution and Al-MB mixture, the decreased absorbency at 664 nm was 0.071 and 0.248, respectively. According to the Lambert – Bear Law, the ratio of absorbency variation in MB solutions is equal to the ratio of the MB concentration variation.[20] For the ultrasonic cavitation, it is also equal to the ratio of the cavitation level variation.[15] Thus, in contrast to the pure MB solution, the cavitation level in the Al-MB mixture increases 3.49 times.

It is commonly acknowledged that particles in water enhance the ultrasonic cavitation yield.[6,7] Therefore, in comparison with the pure MB solution, the cavitation level in particles-water mixture is enhanced. However, the enhancement of cavitation level varies with the surface roughness of particles. Particles with rough surfaces facilitate the entrapment and the stabilization of gas nuclei.[21] As shown in Fig. 1(b), the crevices on the surface of Al particles will facilitate capturing and stabilizing the gas nuclei. Therefore, in contrast to SiC particles and Al_2O_3 particles, Al particles noticeably enhance the ultrasonic cavitation level.

Based above discussion, Al particles are able to inhibit the appearance of microjet-pits on carbon steel, but not the plastic protuberances due to the impact of shockwave generated in the collapse of cavitation bubbles.[11] Thus, the collapse of cavitation bubbles has not been interfered by Al particles. The high ultrasonic cavitation level in Al-water mixture also supports this conclusion (Fig. 6(b)). Because the microjet-pits are due to the collapse of cavitation bubble near or directly contact with the solid surface,[22] the impact process of microjet on the surface of specimen may have been interfered by Al particles. We proposed that Al particles might play a role more than just providing nucleation sites for the cavitation bubbles. Al particles may make cavitation bubbles to collapse at adequate large distance away from the surface of specimen, because the impact of microjet on the solid surface will be destructive when bubbles collapse close to the solid surface.[23] Since the shockwave can propagate in the water, thus even Al particles cause the cavitation bubbles to collapse at a place where is relative far away from the surface of carbon steel, the shockwave is still able to cause plastic deformation on the carbon steel.

If this proposition is right, what is the correlation between the inhibition of microjet-pits on the carbon steel and the high cavitation level in the particle-water mixture? In contrast to the smooth surfaces of SiC particles and Al_2O_3 particles, the lamellar surfaces of Al particles provide abundant crevices and high specific surface area for gas nuclei to grow into cavitation bubbles, gas nuclei on the surface of these particles are the weakest point of tensile strength in the particle-water mixture.[2]

Thus, cavitation bubbles will mainly grow from the surfaces of these particles. Then, collapse position of the cavitation bubbles may be affected by the position and the movement of these particles in water. Li et al.[24] discovered that the long range repulsive electrostatic double layer interaction between SiO_2 particles and the surface of aluminum bronze in water had an effect on preventing SiO_2 particles approaching the surface of aluminum bronze. If such repulsive interaction also exist between Al particles and the surface of AISI 1045 steel, the larger distance between the collapsing bubbles and the solid surface will attenuate the impact of microjet even cavitation bubbles collapse. Despite the evidence to support this model is still lacking, the anti microjet-pits capacity of Al particles in the hybrid particles-water mixture can be explained based on this model. Because Al particles are more suitable to carry gas nuclei than SiC or Al_2O_3 particles, when Al particles and SiC particles or Al_2O_3 particles mix, the gas nuclei may still tend to exist on Al particles. As a result, Al may still dominate whether the microjet-pits will form or not even other particles exist in the mixture. While, other than the surface morphology, the surface property of particles, such as surface hydrophobicity, may also affects the capture and the stabilization of gas nuclei on particles.[21] That explains why the anti micro-jet pits capacity of Al/Al_2O_3-water mixture is worse than that of Al/SiC-water mixture. Actually, due to the oxidation on Al particles, a thin oxide layer formed on Al particles. Thus, from the chemical perspective, Al_2O_3 particles are more similar to Al particles than SiC particles.

IV. CONCLUSIONS

In summary, the significant inhibition of microjet-pits on carbon steel (AISI 1045) was discovered in the Al/Al_2O_3-water mixtures with a strong cavitation yield. On the contrary, the plastic deformation due to the impact of shockwave has not been noticeably affected by Al particles. The microjet-pits were also inhibited in the Al/SiC and Al/Al_2O_3 hybrid water mixtures, though Al_2O_3 particles weakened the anti microjet-pits capacity of Al particles. Though the underlying mechanism was still obscure, we proposed that the unique surface morphology and surface chemical property of Al particles might make most gas nuclei existing on Al particles and collapse at a relative far distance from the surface of carbon steel. As a result, the microjet energy were attenuated too low to form the needle like pits on carbon steel. In addition, because the microjet-pits on carbon steel are noticeably inhibited in Al-H_2O mixture, this study provided a promising route to investigate the ultrasonic cavitation erosion on the carbon steel merely due to the shockwave, which might facilitate further study on the mechanism of cavitation erosion.

ACKNOWLEDGEMENT

This work was supported by the National Natural Science Foundation of China Project under grant nos. 51375253 and 51321092.

[1] Haosheng Chen, Shihan Liu, Jiadao Wang, and Darong Chen, Journal of applied physics **101**(10), 103510 (2007).
[2] Kenneth Sanders Suslick, *Ultrasound: its chemical, physical, and biological effects* (VCH Publishers, 1988).
[3] Anthony A Atchley and Andrea Prosperetti, The Journal of the Acoustical Society of America **86**(3), 1065 (1989).
[4] HB Marschall, Knud Aage Mørch, AP Keller, and M Kjeldsen, Physics of Fluids (1994-present) **15**(2), 545 (2003).
[5] Manish Arora, Claus-Dieter Ohl, and Knud Aage Mørch, Physical review letters **92**(17), 174501 (2004).
[6] Toru Tuziuti, Kyuichi Yasui, Manickam Sivakumar, Yasuo Iida, and Norio Miyoshi, The Journal of Physical Chemistry A **109**(21), 4869 (2005).
[7] Toru Tuziuti, Kyuichi Yasui, Teruyuki Kozuka, Atsuya Towata, and Yasuo Iida, The Journal of Physical Chemistry A **111**(48), 12093 (2007).
[8] Haosheng Chen, Jiadao Wang, and Darong Chen, Wear **266**(1), 345 (2009).
[9] Si Huang, Akio Ihara, Hideo Watanabe, and Hiroyuki Hashimoto, Journal of fluids engineering **118**(4), 749 (1996).
[10] VI Zmij, GN Kartmazov, NF Kartsev, Yu V Kunchenko, LS Ozhigov, and SG Ruden'kij, (2010).
[11] A Abouel-Kasem, A Ezz El-Deen, KM Emara, and SM Ahmed, Journal of Tribology **131**(3), 031605 (2009).
[12] Haosheng Chen, Wear **269**(7), 602 (2010).
[13] Dayun Yan, Jiadao Wang, Fengbin Liu, and Darong Chen, Wear **303**(1), 419 (2013).
[14] P Riesz, D Berdahl, and CL Christman, Environmental Health Perspectives **64**, 233 (1985).
[15] M Haluzik, J Nedvidkova, and J Skrha, Physiological research **47**, 337 (1998).
[16] Xiaodong ZHANG, Yong FU, Zhiyi LI, and Zongchang ZHAO, Chinese Journal of Chemical Engineering **16**(4), 547 (2008).
[17] SA Karrab, MA Doheim, Mohamed S Mohammed, and SM Ahmed, Tribology letters **45**(3), 437 (2012).

[18] EE Oguzie, Materials Letters **59**(8), 1076 (2005).
[19] Shihan Liu and Daring CHEN, Acta Metallurgica Sinica **45**(5), 519 (2009).
[20] F Li and HL Zheng, Guang pu xue yu guang pu fen xi = Guang pu **26**(12), 2294 (2006).
[21] Bram M Borkent, Manish Arora, and Claus-Dieter Ohl, The Journal of the Acoustical Society of America **121**(3), 1406 (2007).
[22] A Philipp and W Lauterborn, Journal of Fluid Mechanics **361**, 75 (1998).
[23] HS Chen, JD Wang, YJ Li, and DR Chen, Proceedings of the Institution of Mechanical Engineers, Part J: Journal of Engineering Tribology **222**(4), 523 (2008).
[24] Jiang Li, Haosheng Chen, and Fengbin Liu, Applied Surface Science **258**(1), 474 (2011).